JOURNAL OF GUIDANCE, CONTROL, AND DYNAMICS
Vol. 28, No. 4, July–August 2005

Engineering Notes

ENGINEERING NOTES are short manuscripts describing new developments or important results of a preliminary nature. These Notes should not exceed 2500 words (where a figure or table counts as 200 words). Following informal review by the Editors, they may be published within a few months of the date of receipt. Style requirements are the same as for regular contributions (see inside back cover).

Model Predictive Control of a Parafoil and Payload System

Nathan Slegers* and Mark Costello†
Oregon State University, Corvallis, Oregon 97331

Nomenclature

$\bar{b}, \bar{c}, \bar{d}$	=	parafoil span, parafoil chord, and control flap width
$C_{D0}, C_{D\alpha 2}, C_{D\delta a}$	=	aerodynamic drag coefficients for parafoil and payload
$C_{L0}, C_{L\alpha}, C_{L\delta a}$	=	aerodynamic lift coefficients for parafoil and payload
$C_{l\phi}, C_{lp}, C_{l\delta a}$	=	aerodynamic roll coefficients for parafoil and payload
$C_{m0}, C_{m\alpha}, C_{mq}$	=	aerodynamic pitch coefficients for parafoil and payload
$C_{nr}, C_{n\delta a}$	=	aerodynamic yaw coefficients for parafoil and payload
F_A	=	aerodynamic force components in body reference frame
F_W	=	combined weight force components of parafoil and payload in body frame
H_p	=	prediction horizon
I_T	=	inertia matrix of combined parafoil and payload system with respect to its mass center
m_T	=	combined mass of payload and parafoil
p, q, r	=	components of angular velocity of system in body reference frame
S_ω	=	skew symmetric cross-product operator of parafoil and payload system angular velocity
T	=	transformation matrix from inertial to body reference frame
V_A	=	total aerodynamic velocity of parafoil and payload system
x, y, z	=	components of position vector of mass center in inertial frame
$\dot{x}, \dot{y}, \dot{z}$	=	components of velocity vector of mass center in inertial frame
δ_{bias}	=	control bias
σ	=	intersect parameter defining second point in desired path
ϕ, θ, ψ	=	Euler roll, pitch, and yaw angles

I. Introduction

PARAFOIL and payload systems are lightweight, fly at low speed, provide soft landing capability, and are compact before deployment. The dynamics are sufficiently slow so that expert paraglider pilots can track a desired trajectory and attain accurate ground impact. Subconsciously, these pilots continuously project the trajectory forward in time and compare the results with the desired path. The error between the projected and desired path is used to determine control action. A control strategy that mimics how human pilots control paragliders is model predictive control. In model predictive control, a dynamic model of the system is used to project the state into the future and subsequently use the estimated future states to determine control action. It is a common control technique in the process control industry. The basic theory is detailed by Ikonen and Najim.[1] Currently, model predictive control is being applied to a wide variety of problems, spanning many different industries. Mei et al.[2] studied vibration reduction of a tall building experiencing wind excitation using model predictive control and linear quadratic Gaussian control strategies. They found that the model predictive control scheme performed well and was robust to uncertainty in building stiffness. Tsai and Huang[3] used a model reference adaptive predictive controller for a variable-frequency oil-cooling machine used with a dynamically complex machine tool. Kvaternik et al.[4] developed a generalized predictive controller for tilt rotor aeroelastic stability augmentation in an airplane mode of flight. When the model predictive control strategy was used, significant increases in damping of aircraft flexible vibration modes were achieved in a wind-tunnel test.

Substantial research has been reported on the dynamics of parafoils and payloads, beginning with that of Ware and Hassell,[5] who investigated ram-air parachutes in a wind tunnel. Flight tests have been more recently reported on NASA's X-38 (Refs. 6 and 7) parafoil, investigating the lateral and longitudinal aerodynamics for large-scale parafoils. Parafoil dynamic model complexity varies significantly in the literature with simple three- and four-degrees-of-freedom (DOF) models by Jann,[8] a six-DOF model by Mortaloni et al.,[9] and a nine-DOF model from Slegers and Costello.[10] The accuracy of all parafoil dynamic models relies on estimation of aerodynamic coefficients and subsequent verification of the model with flight data. System identification of parafoil aerodynamics varies significantly in the literature with Hur and Valasek[11] using an observer kalman filter identification methodology, Rogers[12] using an extended Kalman filter, and Jann[8] using a Gauss–Newton optimization method.

The work reported here creates a model predictive control strategy for a parafoil and payload aircraft. The standard model predictive control strategy is modified to account for brake deflection bias, which is significant because subtle changes in the parafoil canopy that naturally occur from flight to flight cause significant brake deflection bias. A simplified six-DOF model is presented and used as a basis for a reduced-order linear model used in the model predictive control strategy. The reduced-order linear model maintains only information that is most significant to the performance of the controller. System identification is performed using

Presented as Paper 2004-4822 at the AIAA Atmospheric Flight Mechanics Conference, Providence, RI, 16–19 August 2004; received 15 July 2004; revision received 27 December 2004; accepted for publication 28 December 2004.

*Research Associate, Department of Mechanical Engineering. Member AIAA.

†Associate Professor, Department of Mechanical Engineering. Member AIAA.

a recursive weighted least-squares method. Performance of the autonomous flight control system is shown through flight tests of the system under a variety of conditions.

II. Model Predictive Control

Consider a discrete system described in state-space form:

$$x_{k+1} = Ax_k + Bu_k + D, \qquad y_k = Cx_k \tag{1}$$

Assume that the system matrices A, B, C, and D are known and that x_k is the state vector, u_k is the control input, and y_k is the output at time k. The discrete model can be used to estimate the future state of the system. Under the assumption that a desired trajectory is known (w_k), an estimated error signal $\tilde{e}_k = w_k - \tilde{y}_k$ is computed over a finite set of future time instants called the prediction horizon H_p. The tilde is used to represent an estimated quantity. In model predictive control, the control computation problem is cast as a finite time discrete optimal control problem. To compute the control input at a given time instant, a quadratic cost function is minimized through the selection of the control history over the control horizon. The cost function can be written as

$$J = (W - \tilde{Y})^T(W - \tilde{Y}) + U^T RU \tag{2}$$

where

$$W = \begin{bmatrix} w_{k+1} & w_{k+2} & \cdots & w_{k+H_p} \end{bmatrix}^T \tag{3}$$

$$\tilde{Y} = K_{CA}x_k + K_{CAB}U + K_{CAD} \tag{4}$$

$$U = \begin{bmatrix} u_k & u_k & \cdots & u_{k+H_p-1} \end{bmatrix}^T \tag{5}$$

and R is a symmetric positive semidefinite matrix of size H_p:

$$K_{CA} = \begin{bmatrix} CA \\ CA^2 \\ \vdots \\ CA^{HP} \end{bmatrix} \tag{6}$$

$$K_{CAB} = \begin{bmatrix} CB & 0 & 0 & 0 & 0 \\ CAB & CB & 0 & 0 & 0 \\ CA^2B & CAB & CB & 0 & 0 \\ \vdots & \vdots & & \ddots & 0 \\ CA^{H_p-1}B & \cdots & CA^2B & CAB & CB \end{bmatrix} \tag{7}$$

$$K_{CAD} = \begin{bmatrix} CD \\ CAD + CD \\ CA^2D + CAD + CD \\ \vdots \\ CA^{H_p-1}D + CA^{H_p-2} + \cdots + CD \end{bmatrix} \tag{8}$$

Equation (4) is substituted into Eq. (2), resulting in the cost function in Eq. (9) that is in terms of the system state x_k, desired trajectory W, control vector U, and system matrices A, B, C, D, and R,

$$\begin{aligned} J = {} & (W - K_{CA}x_k - K_{CAB}U - K_{CAD})^T(W - K_{CA}x_k \\ & - K_{CAB}U - K_{CAD}) + U^T RU \end{aligned} \tag{9}$$

The control U, which minimizes Eq. (9), is

$$U = K(W - K_{CA}x_k - K_{CAD}) \tag{10}$$

where

$$K = \left(K_{CAB}^T K_{CAB} + R\right)^{-1} K_{CAB}^T \tag{11}$$

Equation (10) contains the optimal control inputs over the entire control horizon; however, at time k, only the first element u_k is needed. The first element u_k is extracted from Eq. (10) by defining K_1 as the first row of K. The optimal control over the next time sample becomes

$$u_k = K_1(W - K_{CA}x_k - K_{CAD}) \tag{12}$$

where calculation of the first element of the optimal control sequence requires the desired trajectory W over the prediction horizon and the current state x_k.

III. Parafoil and Payload Model

The combined system of the parafoil canopy and the payload is represented with six DOF, including three inertial position components of the system mass center as well as the three Euler orientation angles of the parafoil and payload system. Kinematic equations of motion for the parafoil and payload system are

$$\begin{Bmatrix} \dot{x} \\ \dot{y} \\ \dot{z} \end{Bmatrix} = T^T \begin{Bmatrix} u \\ v \\ w \end{Bmatrix} \tag{13}$$

$$\begin{Bmatrix} \dot{\phi} \\ \dot{\theta} \\ \dot{\psi} \end{Bmatrix} = \begin{bmatrix} 1 & s_\phi t_\theta & c_\phi t_\theta \\ 0 & c_\phi & -s_\phi \\ 0 & s_\phi/c_\phi & c_\phi/c_\theta \end{bmatrix} \begin{Bmatrix} p \\ q \\ r \end{Bmatrix} \tag{14}$$

The matrix T represents the transformation matrix from an inertial reference frame to the body reference frame:

$$T = \begin{bmatrix} c_\theta c_\psi & c_\theta s_\psi & -s_\theta \\ s_\phi s_\theta c_\psi - c_\phi s_\psi & s_\phi s_\theta s_\psi + c_\phi c_\psi & c_\theta s_\phi \\ c_\phi s_\theta c_\psi + s_\phi s_\psi & c_\phi s_\theta s_\psi - s_\phi c_\psi & c_\phi c_\theta \end{bmatrix} \tag{15}$$

The common shorthand notation for trigonometric functions is employed where $\sin(\alpha) \equiv s_\alpha$, $\cos(\alpha) \equiv c_\alpha$, and $\tan(\alpha) \equiv t_\alpha$. The dynamic equations of motion are

$$\begin{Bmatrix} \dot{u} \\ \dot{v} \\ \dot{w} \end{Bmatrix} = \frac{1}{m_T}(F_A + F_W) - TS_\omega T^T \begin{Bmatrix} u \\ v \\ w \end{Bmatrix} \tag{16}$$

$$\begin{Bmatrix} \dot{p} \\ \dot{q} \\ \dot{r} \end{Bmatrix} = I_T^{-1}\left(M_A - S_\omega I_T \begin{Bmatrix} p \\ q \\ r \end{Bmatrix}\right) \tag{17}$$

where

$$S_\omega = \begin{bmatrix} 0 & -r & q \\ r & 0 & -p \\ -q & p & 0 \end{bmatrix} \tag{18}$$

$$I_T = \begin{bmatrix} I_{XX} & 0 & I_{XZ} \\ 0 & I_{YY} & 0 \\ I_{XZ} & 0 & I_{ZZ} \end{bmatrix} \tag{19}$$

$$I_T^{-1} = \begin{bmatrix} I_{XXI} & 0 & I_{XZI} \\ 0 & I_{YYI} & 0 \\ I_{XZI} & 0 & I_{ZZI} \end{bmatrix} \tag{20}$$

The weight force vector in the body reference frame is

$$F_W = m_T g \begin{Bmatrix} -s_\theta \\ s_\phi c_\theta \\ c_\phi c_\theta \end{Bmatrix} \tag{21}$$

The aerodynamic forces acting at the system mass center and the aerodynamic moments about the system mass center are given in Eqs. (22) and (23), respectively. $C_{l\phi}$ is introduced to eliminate the center of pressure location from the dynamic equations while maintaining the parafoils tendency to glide with no roll during neutral control.

$$F_A = \frac{1}{2}\rho S V_A (C_{L0} + C_{L\alpha}\alpha + C_{L\delta a}\delta_a) \begin{Bmatrix} w \\ 0 \\ -u \end{Bmatrix} - \frac{1}{2}\rho S V_A \left(C_{D0} + C_{D\alpha 2}\alpha^2 + C_{D\delta a}\delta_a\right) \begin{Bmatrix} u \\ v \\ w \end{Bmatrix} \tag{22}$$

$$M_A = \frac{1}{2}\rho S V_A^2 \begin{Bmatrix} C_{l\phi}\bar{b}\phi + \dfrac{C_{lp}\bar{b}^2 p}{2V_A} + \dfrac{C_{l\delta a}\delta_a \bar{b}}{\bar{d}} \\ C_{m0}\bar{c} + C_{m\alpha}\bar{c}\alpha + \dfrac{C_{mq}\bar{c}^2 q}{2V_A} \\ \dfrac{C_{nr}\bar{b}^2 r}{2V_A} + \dfrac{C_{n\delta a}\bar{b}\delta_a}{\bar{d}} \end{Bmatrix} \tag{23}$$

Model predictive control requires a linear model of the states to be controlled. The desired states to control in a parafoil and payload system are the inertial positions x and y. Equations (13–23) describing the parafoil and payload system are nonlinear and, to apply standard model predictive control, must be linearized. Consider a parafoil and payload in a steady turn performing a helix as it falls. All of the states excluding the inertial positions x, y, and z and Euler yaw angle reach a steady state. The inertial positions do not appear in any of the equations of motion. However, yaw angle appears in Eq. (13) relating inertial velocities to body velocities. A linear six-DOF model that accurately represents the inertial position of the nonlinear model must constrain the yaw angle to only small changes about a nominal yaw angle. Constraining the yaw angle in such a way limits the model to nearly straight flight and is not sufficient for general flight. Observation of a parafoil and payload system shows that the velocities u, v, and w expressed in the body reference frame are nearly constant under typical flight conditions. If a reduced state $[\phi \;\; \psi \;\; p \;\; r]^T$ is considered for model predictive control purposes, then the equations for $[\dot{\phi} \;\; \dot{\psi} \;\; \dot{p} \;\; \dot{r}]^T$ describing the rolling and pitching in Eqs. (14) and (17) can be linearized assuming that the aerodynamic velocity V_A is constant. Euler pitch angle is not included in the reduced state because after linearization pitch angle becomes uncoupled from both rolling and yawing motion. The equations for the reduced states are linearized about the steady state:

$$\begin{Bmatrix} \delta\dot{\phi} \\ \delta\dot{\psi} \\ \delta\dot{p} \\ \delta\dot{r} \end{Bmatrix} = \begin{bmatrix} 0 & 0 & 1 & 0 \\ 0 & 0 & 0 & 1/c_{\theta_0} \\ \dfrac{\rho S\bar{b}V_A^2 I_{XXI} C_{l\phi}}{2} & 0 & \dfrac{\rho S\bar{b}^2 V_A I_{XXI} C_{lp}}{4} & \dfrac{\rho S\bar{b}^2 V_A I_{XZI} C_{nr}}{4} \\ \dfrac{\rho S\bar{b}V_A^2 I_{XZI} C_{l\phi}}{2} & 0 & \dfrac{\rho S\bar{b}^2 V_A I_{XZI} C_{lp}}{4} & \dfrac{\rho S\bar{b}^2 V_A I_{ZZI} C_{nr}}{4} \end{bmatrix} \times \begin{Bmatrix} \delta\phi \\ \delta\psi \\ \delta p \\ \delta r \end{Bmatrix} + \begin{bmatrix} 0 \\ 0 \\ \dfrac{\rho S\bar{b}V_A^2 (C_{l\delta a} I_{XXI} + C_{n\delta a} I_{XZI})}{2\bar{d}} \\ \dfrac{\rho S\bar{b}V_A^2 (C_{l\delta a} I_{XZI} + C_{n\delta a} I_{ZZI})}{2\bar{d}} \end{bmatrix} \{\delta_a\} + \begin{bmatrix} 0 \\ 0 \\ \dfrac{\rho S\bar{b}V_A^2 I_{XZI}}{2\bar{d}} \\ \dfrac{\rho S\bar{b}V_A^2 I_{ZZI}}{2\bar{d}} \end{bmatrix} \{\delta_{\text{bias}}\} \tag{24}$$

A typical desired trajectory of a parafoil and payload system consist of points in the x–y plane, and, according to Eq. (1), the desired output must be a linear combination of the linear model states. To use the linear model described in Eq. (24) for model predictive control, the desired trajectory in the x–y plane must be mapped into a desired trajectory in terms of the reduced states $[\phi \;\; \psi \;\; p \;\; r]^T$. A straightforward mapping is to assume that the side velocity v is small, that the parafoil is traveling in the direction of its heading ψ, and that the forward velocity is constant. A desired path defined by points can then be converted to desired heading angle using parametric Lagrange interpolating polynomials.

IV. Test System

The parafoil and payload system used in all testing is shown in Figs. 1 and 2 with the physical parameters in Table 1. A test flight commences by launching the system from the ground. A 10-in. propeller powers the test system to altitudes of from 250 to 400 ft, where the propeller is stopped and gliding commences, lasting approximately 20 s for every 100 ft of altitude.

Full-state measurement of the parafoil required in the optimal control sequence is achieved through a sensor package that includes three single-axis gyroscopes, a three-axis accelerometer, and a three-axis magnetometer. Inertial positions x and y required in the mapping of the desired x–y path into a desired yaw angle are obtained from a wide area augmentation system enabled global positioning satellite receiver. The sensors are supplemented with a wireless transceiver that transmits data from the parafoil and receives commands during flight. An operator-controlled transmitter switches control of the parafoil to one of three modes: manual, estimation, or autonomous. Manual mode allows the operator to fly the parafoil manually. Estimation mode allows estimation of linear

Table 1 Parafoil and payload physical parameters

Variable	Value	Unit
ρ	0.0023784722	slug/ft^3
Weight	2.0	lbf
S	7.5	ft^2
$\bar{b}$	4.25	ft
$\bar{d}$	2.0	ft
I_{XX}	0.1357	slug/ft^2
I_{YY}	0.1506	slug/ft^2
I_{ZZ}	0.0203	slug/ft^2
I_{XZ}	0.0025	slug/ft^2
I_{XXI}	7.3845	ft^2/slug
I_{YYI}	6.6423	ft^2/slug
I_{ZZI}	49.442	ft^2/slug
I_{XZI}	−0.9032	ft^2/slug
V_A	21.6	ft/s

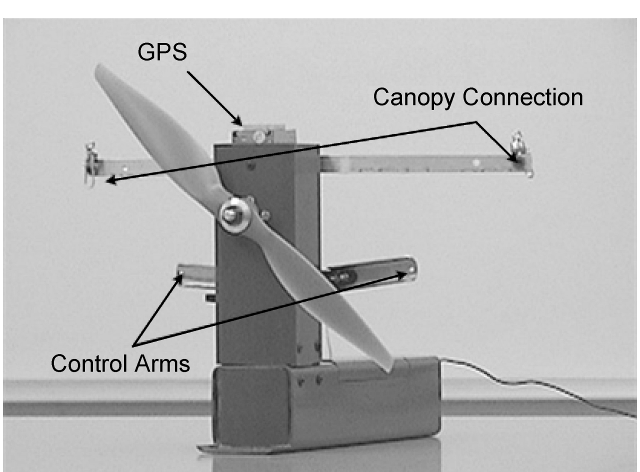

Fig. 1 Payload.

Fig. 2 Parafoil and payload system.

model aerodynamic coefficients required for model predictive control. Autonomous mode controls the parafoil using the model predictive control law.

V. Identification of Aerodynamic Coefficients

Application of the reduced-order model requires knowledge of five constant aerodynamic coefficients, $C_{l\phi}$, C_{lp}, $C_{l\delta a}$, C_{nr}, and $C_{n\delta a}$, and the constant bias term δ_{bias}. The six parameters are estimated using recursive weighted least-squares estimation, where z_i are measurements, $\boldsymbol{x}_i$ are parameters to be estimated, and $\boldsymbol{n}_i$ is zero mean measurement noise:

$$z_i = H_i \boldsymbol{x} + \boldsymbol{n}_i \tag{25}$$

The recursive weighted least-squares estimation to Eq. (25) is given in Eqs. (26) and (27), where P_i is the error covariance estimate of the parameters at measurement i and Q is the measurement noise covariance,[13]

$$\hat{x}_i = \hat{x}_{i-1} + P_i H_i^T Q^{-1}(z_i - H_i \hat{x}_i) \tag{26}$$

$$P_i = P_{i-1} - P_{i-1} H_i^T \left(Q + H_i P_{i-1} H_i^T\right)^{-1} H_i P_{i-1} \tag{27}$$

The matrix H_i yields a linear relationship between the parameters to be estimated, and measurements are acquired by linearizing δp and δ_r in Eq. (24):

$$H_i = \frac{\rho S \bar{b} V_A^2}{2} \begin{bmatrix} I_{XXI}\phi_i & I_{XZI}\phi_i \\ I_{XXI}\dfrac{\bar{b} p_i}{2V_A} & I_{XZI}\dfrac{\bar{b} p_i}{2V_A} \\ I_{XXI}\dfrac{\delta_a}{\bar{d}} & I_{XZI}\dfrac{\delta_a}{\bar{d}} \\ I_{XZI}\dfrac{\bar{b} r_i}{2V_A} & I_{ZZI}\dfrac{\bar{b} r_i}{2V_A} \\ I_{XZI}\dfrac{\delta_a}{\bar{d}} & I_{ZZI}\dfrac{\delta_a}{\bar{d}} \\ \dfrac{I_{XZI}}{\bar{d}} & \dfrac{I_{ZZI}}{\bar{d}} \end{bmatrix}^T$$

The recursive weighted least-squares estimation requires differentiation of measured roll and yaw rates. The control sequence used in parameter identification was chosen to be sinusoidal to ensure that numerical differentiation of roll and yaw rates produced significant signals. Measured roll and yaw rates are processed with a zero-phase digital filter before differentiation. The recursive weighted least-squares estimation is initialized with P_1 as a 6×6 diagonal matrix with 0.05 along the diagonal and $C_{l\phi}$, C_{lp}, $C_{l\delta a}$, C_{nr}, $C_{n\delta a}$, and δ_{bias} as −0.1, −0.5, 0.1, −0.1, 0.1, and 0.0, respectively. The measurement noise covariance Q was set as a 2×2 diagonal matrix with

Table 2 Estimated model coefficients

Parameter	Value
$C_{l\phi}$	−0.0100
C_{lp}	−0.0520
$C_{l\delta a}$	0.0021
C_{nr}	−0.0850
$C_{n\delta a}$	0.0010
δ_{bias}	−0.0001

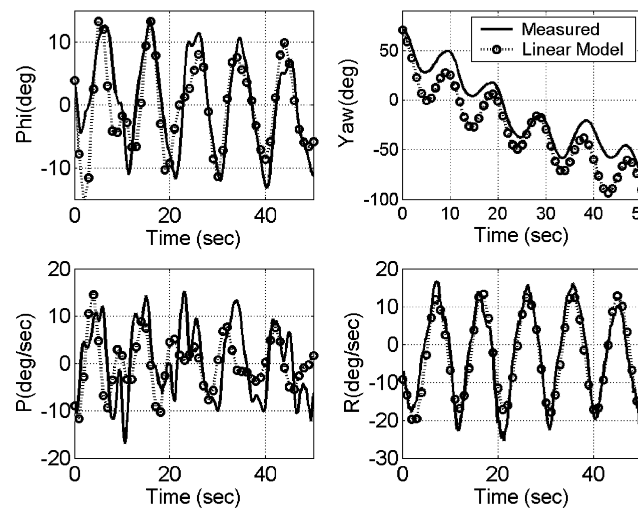

Fig. 3 Comparison of measurement and model.

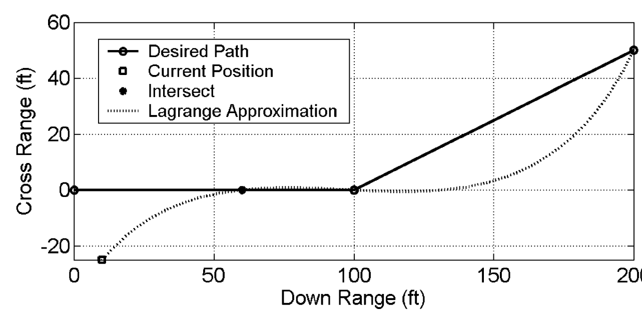

Fig. 4 Lagrange approximating polynomial.

$Q_{1,1} = 0.00475$ and $Q_{2,2} = 0.0005$. The estimated aerodynamic coefficients, $C_{l\phi}$, C_{lp}, $C_{l\delta a}$, C_{nr}, $C_{n\delta a}$, and δ_{bias} from the flight data are given in Table 2. The discrete time linear reduced-order model is verified by comparing simulated results using the estimated aerodynamic coefficients with measured flight data. Figure 3 shows that the reduced-order model is able to capture the fundamental dynamics of the parafoil and payload.

VI. Model Predictive Control Results

The prediction of desired heading angle with third-order Lagrange interpolating polynomials is accomplished using four desired path points. The first point is defined as the current position of the parafoil and payload system. The second point is defined as the location along the desired path that is a distance σ ahead of the current position and is called the intersect parameter. The third and fourth points are the next two desired path points. Figure 4 shows a desired path and the Lagrange interpolating polynomial found. The update rate of the model predictive controller was chosen to be 1 s, and the linear model is converted to a discrete time system of the form in Eq. (1) with a sampling period of 1 s. The discrete time system matrices A, B, C, and D required for the model predictive controller are

$$A = \begin{bmatrix} 0.5243 & 0 & 0.5823 & 0.0100 \\ 0.0120 & 1.0000 & 0.0125 & 0.1372 \\ -0.7589 & 0 & 0.1360 & 0.0047 \\ 0.0056 & 0 & 0.0148 & 0.0009 \end{bmatrix} \tag{28}$$

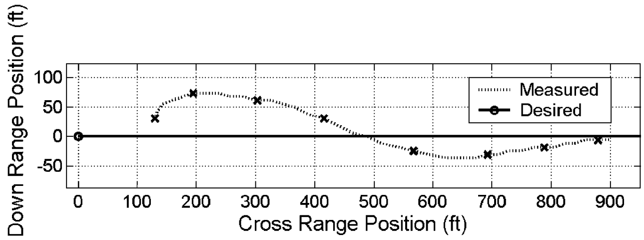

Fig. 5 Controlled straight path (no wind).

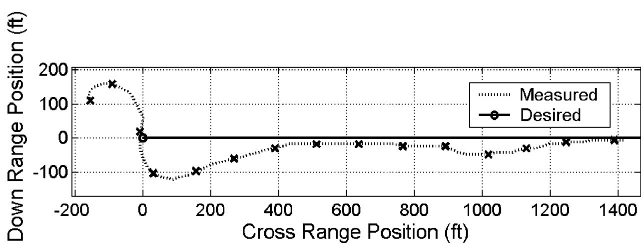

Fig. 6 Controlled straight path (wind).

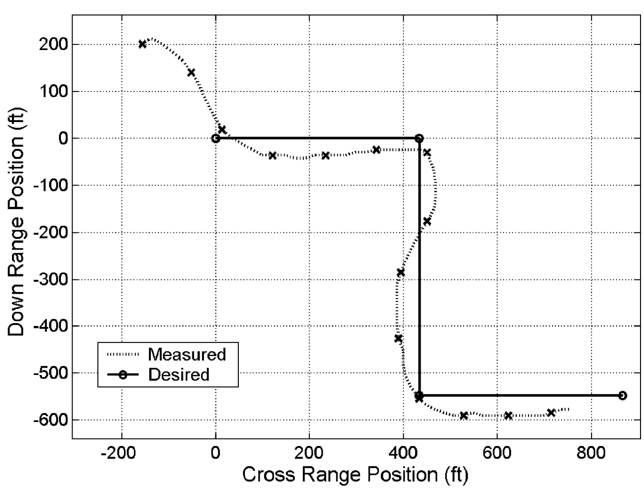

Fig. 7 Controlled S path (no wind).

$$B = \begin{bmatrix} 0.0494 \\ 0.0505 \\ 0.0794 \\ 0.0591 \end{bmatrix} \tag{29}$$

$$C = [0 \quad 1 \quad 0 \quad 0] \tag{30}$$

$$D = \begin{bmatrix} 0.0001 \\ -0.0052 \\ 0.0000 \\ -0.0060 \end{bmatrix} \tag{31}$$

The matrix R penalizing control magnitude in the optimal control sequence is selected as an $H_p \times H_p$ matrix with 0.35 on the diagonal and zeros everywhere else. Results for the model predictive controller are shown in Figs. 5–7 with $H_p = 10$ and $\sigma = 100$ ft. Figure 5 shows the measured path of the parafoil and payload compared to a desired straight path with no wind; the markers designate 5-s intervals with the first marker being the initial position at 0. The control sequence is shown in Fig. 8. Control is initiated with the parafoil and payload initially traveling away from the desired path and 40 ft offtrack. The initial control response is large and negative, corresponding to left braking and negative, crossrange. The parafoil has a maximum error of 75 ft at 100 ft downrange, then overshoots the desired by path by 39 ft at -510 ft downrange before a final error of 9 ft at impact. Figure 6 shows the measured path of the parafoil

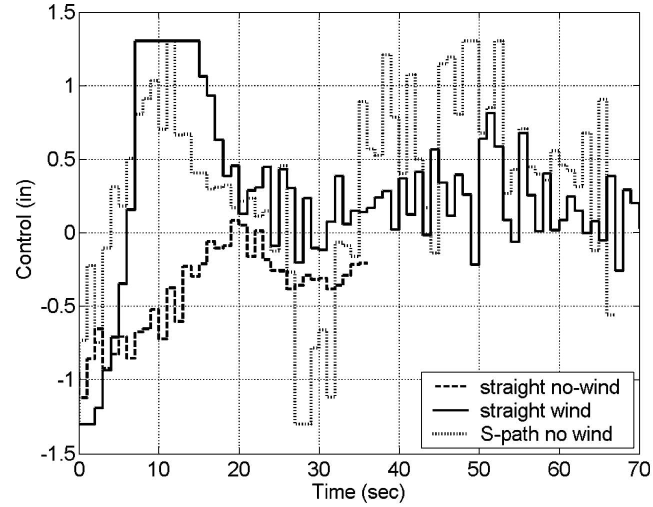

Fig. 8 Control.

and payload compared to the desired straight path and control with a 12-ft/s crosswind from positive to negative crossrange. Control is again shown in Fig. 8 and is initiated with the parafoil and payload initially traveling away from the desired path and 100 ft offtrack. The parafoil has a similar oscillatory response with a maximum error of 119 ft at 230 ft downrange as it overshoots the desired path. The parafoil turns back toward the desired path and comes within 18 ft before the wind pushes it farther away. The final error at impact is 6 ft. The larger error from the crosswind is due to the difference in measured yaw angle and heading angle because of parafoil sideslip. Figure 7 shows the performance of the model predictive controller when tracking the more complicated S-shaped path. Control is initiated when the parafoil and payload are 210 ft offtrack. The maximum error during the flight is 45 ft at 550 ft downrange and -550 ft crossrange. The model predictive controller is able to predict the required control input so that the parafoil and payload system are able to achieve close proximity to the desired points as they are passed.

VII. Conclusions

Model predictive control is a natural way to control a parafoil and payload because it mimics the process that a pilot controlling a paraglider estimates both the path and control sequence to achieve a desired outcome. The work reported here employs model predictive control for autonomous control of a parafoil and payload system. To support the flight control law, a reduced-state linear model was created that uses roll angle, yaw angle, body roll rate, and body yaw rate of the parafoil and payload system. Application of the reduced-order model requires knowledge of five constant aerodynamic coefficients, $C_{l\phi}$, C_{lp}, $C_{l\delta a}$, C_{nr}, and $C_{n\delta a}$, and a constant bias term δ_{bias}. A recursive weighted least-squares estimation is used to estimate the six parameters. The estimated parameters and reduced-state model is compared with flight data, and it is shown that they adequately model the parafoil and payload system. To use the reduced-state linear model, the desired x–y trajectory is mapped into desired yaw angles using Lagrange interpolating polynomials assuming a constant aerodynamic velocity. Three exemplar autonomous flight tests are used to show that model predictive control is an effective way to control autonomously the trajectory of a parafoil and payload system.

References

[1]Ikonen, E., and Najim, K., *Advanced Process Identification and Control*, Marcel Dekker, New York, 2002, pp. 181–197.

[2]Mei, G., Kareem, A., and Kantor, J. C., "Model Predictive Control of Wind-Excited Building: Benchmark Study," *Journal of Engineering Mechanics*, Vol. 130, No. 4, 2004, pp. 459–465.

[3]Tsai, C. C., and Huang, C. H., "Model Reference Adaptive Predictive Control for a Variable-Frequency Oil-Cooling Machine," *IEEE Transactions on Industrial Electronics*, Vol. 51, No. 2, 2004, pp. 330–339.

[4]Kvaternik, R. G., Piatak, D. J., Nixon, M. W., Langston, C. W., Singleton, J. D., Bennett, R. L., and Brown, R. K., "An Experimental Evaluation of Generalized Predictive Control for Tiltrotor Aeroelastic Stability Augmentation in Airplane Mode of Flight," *Journal of the American Helicopter Society*, Vol. 47, No. 3, 2002, pp. 198–208.

[5]Ware, G. M., and Hassell, J. L., Jr., "Wind-Tunnel Investigation of Ram-Air Inflated All-Flexible Wings of Aspect Ratios 1.0 to 3.0," NASA TM SX-1923, 1969.

[6]Iacomini, C. S., and Cerimele, C. J., "Lateral-Directional Aerodynamics from a Large Scale Parafoil Test Program," AIAA Paper 99-1731, 1999.

[7]Iacomini, C. S., and Cerimele, C. J., "Longitudinal Aerodynamics from a Large Scale Parafoil Test Program," AIAA Paper 99-1732, 1999.

[8]Jann, T., "Aerodynamic Model Identification and GNC Design for Parafoil-Load System Alex," AIAA Paper 2001-2015, 2001.

[9]Mortaloni, P., Yakimenko, O., Dobrokhodov, V., and Howard, R., "On the Development of a Six-Degree-of-Freedom Model of a Low-Aspect-Ratio Parafoil Delivery System," AIAA Paper 2003-2105, May 2003.

[10]Slegers, N., and Costello, M., "Aspects of Control for a Parafoil and Payload System," *Journal of Guidance, Control, and Dynamics*, Vol. 26, No. 6, 2003, pp. 898–905.

[11]Hur, G., and Valasek, J., "System Identification of Powered Parafoil-Vehicle from Flight Test Data," AIAA Paper 2003-5539, Aug. 2003.

[12]Rogers, R., "Aerodynamic Parameter Estimation for Controlled Parachutes," AIAA Paper 2002-4708, Aug. 2002.

[13]DeRusso, P., Roy, R., Close, C., and Desrochers, A., *State Variables for Engineers*, 2nd ed., Wiley, New York, 1998, pp. 393–400.